Colloid & Polymer Science Colloid Polym Sci 272: 604–611 (1994)

Electron microscopic and light scattering observation on a system with two iridescent phases

T. Imae, T. Iwamoto[1]), G. Platz[2]), and C. Thunig[2])

Department of Chemistry, Faculty of Science
[1]) Equipment Center for Education and Research, School of Medicine, Nagoya University, Nagoya Japan
[2]) Institut für Physikalische Chemie I der Universität Bayreuth, Bayreuth, FRG

Abstract: Electron microscopic observations and classical light-scattering measurements have been carried out for dodecyldimethylaminoxide/hexanol/water mixtures in the concentration range where iridescent colors occur. This system has two different iridescent phases. The iridescent phase with more hexanol forms quickly, and the phase with less hexanol forms very slowly. Three different isotropic phases which show strong flow birefringence are found near both iridescent phases. The electron microscopic pictures show clearly that only one of these isotropic phases with strong flow birefringence is a bicontinuous sponge phase (L_{3h}-phase). This is the phase which comes out by adding some alkanol to the upper lamellar phase. The flow birefringent phase below the lower lamellar phase forms unilamellar vesicles. The flow birefringent phase which occurs between both iridescent phases contains multilamellar vesicles and is shown to be a precursor of a lamellar phase.

Key words: Electron microscopy – light scattering – dodecyldimethylaminoxide/hexanol/water – iridescent phase – bicontinuous sponge phase – vesicle phase

1. Introduction

It is known that the addition of small amounts of hexanol or other long chain alkanols to binary surfactant/water solutions of alkylaminoxides produces lamellar phases which can be diluted until iridescent colors are found [1]. The system of dodecyldimethylaminoxide (C_{12}DMAO), hexanol, and water is the first and until now the only one which is reported to contain two iridescent phases [2]. One iridescent phase forms quickly at higher hexanol concentrations. The other forms very slowly at lower hexanol concentrations. These iridescent phases are surrounded by isotropic phases with strong shear birefringence (L_3-phases). Electron microscopic observations on similar systems have been recently published [3]. In this work, we compare classical light-scattering measurements and electron microscopic observations of C_{12}DMAO/hexanol/water mixtures in order to characterize molecular assemblies in different phases which occur around the concentration range where the iridescent colors are found.

2. Experimental section

A sample of C_{12}DMAO is the same as previously used [1]. Hexanol is a commercial product. Solutions with 30 and 50 mM C_{12}DMAO and different hexanol concentrations were prepared according to the previous procedure [2] and were allowed to stand for 4 weeks in a 25 °C water bath in order to attain the equilibrium of molecular assemblies. Freeze fracture replica films were prepared on a freeze fracture apparatus, Balzers BAF 400, and electron microscopic observation was performed on a Hitachi electron microscope, H-800.

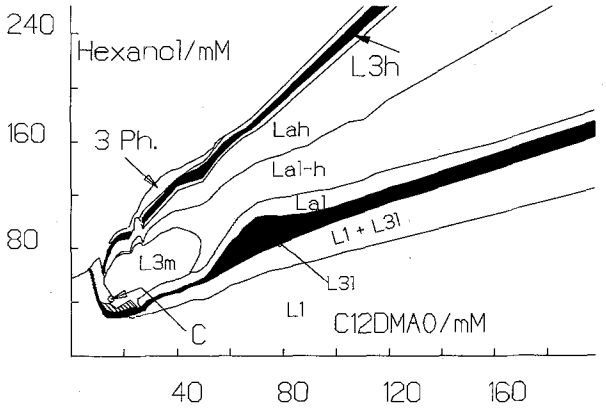

Fig. 1. Phase diagram (dilute region) of the system $C_{12}DMAO/H_2O$/hexanol at 25 °C

Light-scattering measurements have been carried out on the equipment mentioned before [2]. A Zeiss Polarization Microscope was used for optical observations of textures of the lamellar phases.

3. Results

The phase diagram of the $C_{12}DMAO$/hexanol/water ternary system has been examined in detail [2]. Figure 1 shows the phase diagram in the dilute region at 25 °C. The lamellar phases are $L_{\alpha l}$ and $L_{\alpha h}$. The isotropic phases with strong flow birefringence are L_{3h}, L_{3m} and L_{3l} which is also known as L_1^*-phase. The behavior of this phase is much more similar to that of a sponge-phase than that of a L_1-phase. Therefore, we prefer to call this phase L_{3l}-phase.

For the first time after preparation of the solutions nearly the whole region between $L_{\alpha l}$ and $L_{\alpha h}$ looks like the L_{3m}-phase. Yet after a very long time (1 to several months) a phase is apparent which looks like a mixture of both the $L_{\alpha l}$ and the $L_{\alpha h}$ phase ($L_{\alpha l-h}$). No macroscopic separation can be observed in this birefringent region. The phase transformation process starts from higher surfactant concentration regions and the new phase boundary moves with time to lower surfactant concentrations.

Electron micrographs for 30 mM $C_{12}DMAO$/hexanol/water mixtures are given in Fig. 2. A homogeneous solution with 45 mM hexanol (L_{3l}-phase) reveals images of particles with various

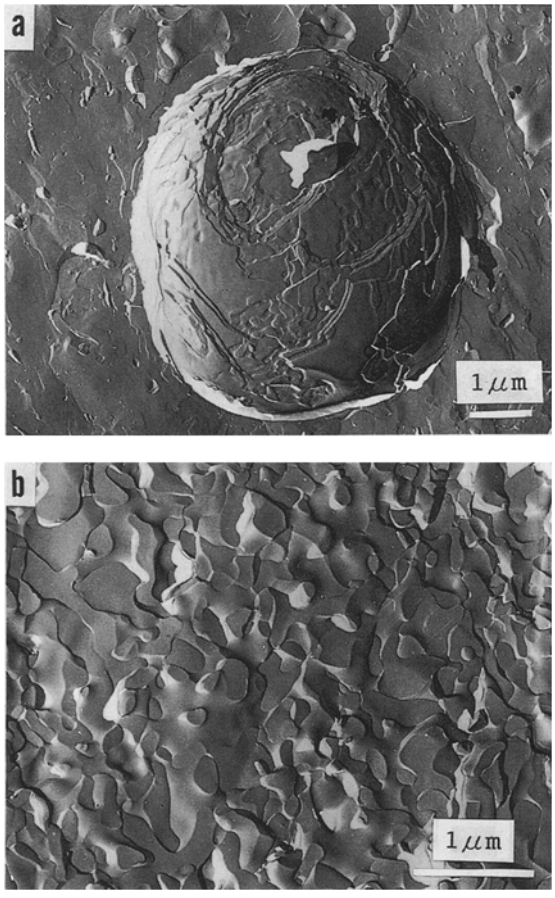

Fig. 2. Electronmicroscopic pictures 30 mM $C_{12}DMAO$ a: 60 mM hexanol; L_{3m}-phase b: 100 mM hexanol; L_{3h}-phase (sponge phase)

sizes less than 700 nm, some of which deviate from spherical shape. In a solution with 60 mM hexanol (L_{3m}-phase), there are globular particles with diameters less than 6 μm (Fig. 2a). Particles have multilamellar layers of 50 nm separation distance. The distance between the lamellar layers within the multilamellar vesicles expands to 110–140 nm at 80 mM hexanol. The region around these multilamellar vesicular particles has no structure which can be well defined by our electronmicroscopic pictures. It seems that there are fragments of broken lamellae with no interlamellar order. The distance between those fragments is in the order of 100–250 nm.

With further addition of hexanol the globular shape and the regions with fragments disappear, and flat lamellar layers of a well defined lamellar

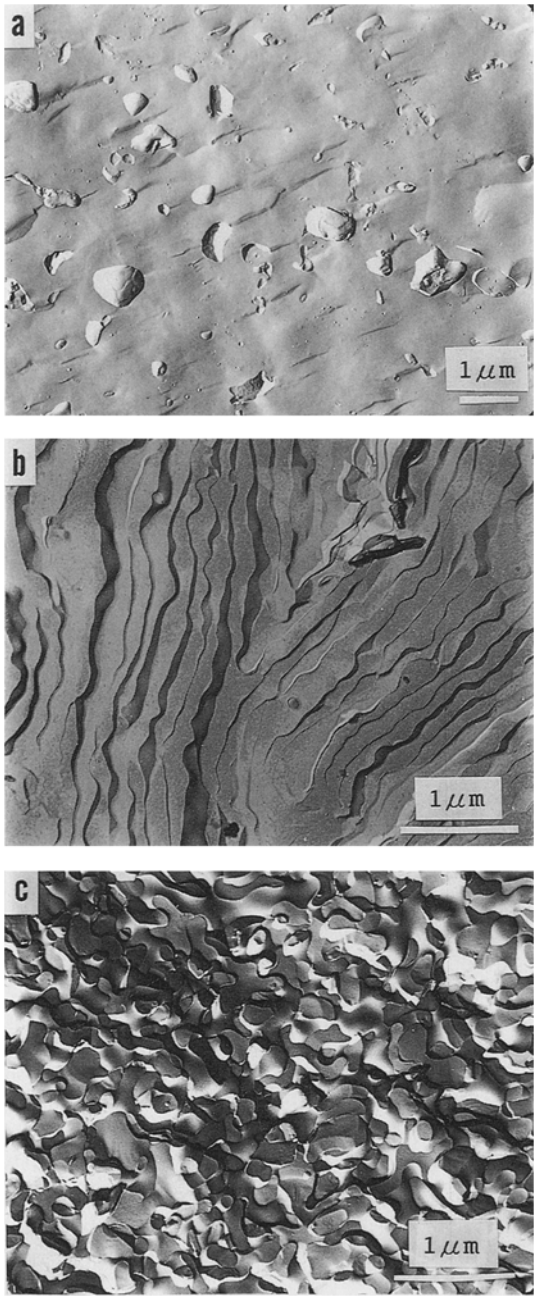

Fig. 3. Electronmicroscopic pictures 50 mM C_{12}DMAO a: 60 mM hexanol; L_{3l}-phase b: 120 mM hexanol; $L_{\alpha h}$-phase c: 140 mM hexanol; L_{3h}-phase

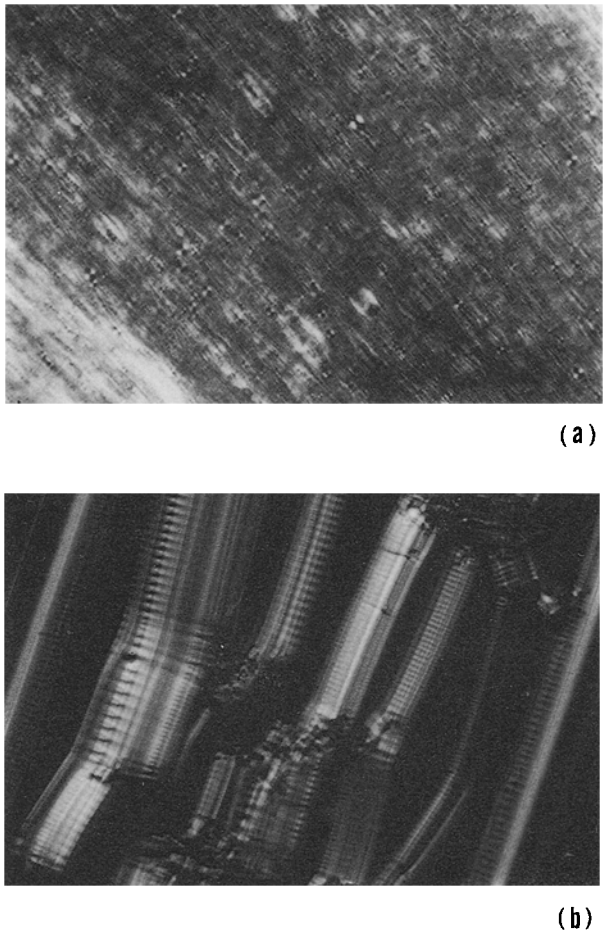

Fig. 4. Polarization micrographs (100-fold) a: $L_{\alpha l}$-phase (100 mM C_{12}DMAO, 120 mM hexanol) b: $L_{\alpha h}$-phase (100 mM C_{12}DMAO, 210 mM hexanol)

phase become dominant. The interlamellar distance is 190–250 nm at 95 mM hexanol.

The structure of the L_{3h}-phase is quite different (Fig. 2b). We can clearly recognize that there are bicontinuous structures of a typical sponge phase in solutions with 97.5 and 100 mM hexanol.

Electron micrographs for aqueous 50 mM C_{12}DMAO solutions with various hexanol concentrations are given in Fig. 3. Particles with various sizes less than 700 nm are observed in solutions of the L_{3l}-phase (Fig. 3a). Some particles take nonspherical shape and capsulate small particles. Above 80 mM hexanol concentration ($L_{\alpha l-h}$-phase), lamellar layers are formed. Lamellar structures are found in the $L_{\alpha l}$-, $L_{\alpha l-h}$- and $L_{\alpha h}$-regions. But only the upper lamellar phase ($L_{\alpha h}$) shows well aligned lamellae with nearly no interlamellar distance fluctuations. The interlamellar spacing evaluated from the electronmicrograph pictures (Fig. 3b) is around 120 nm.

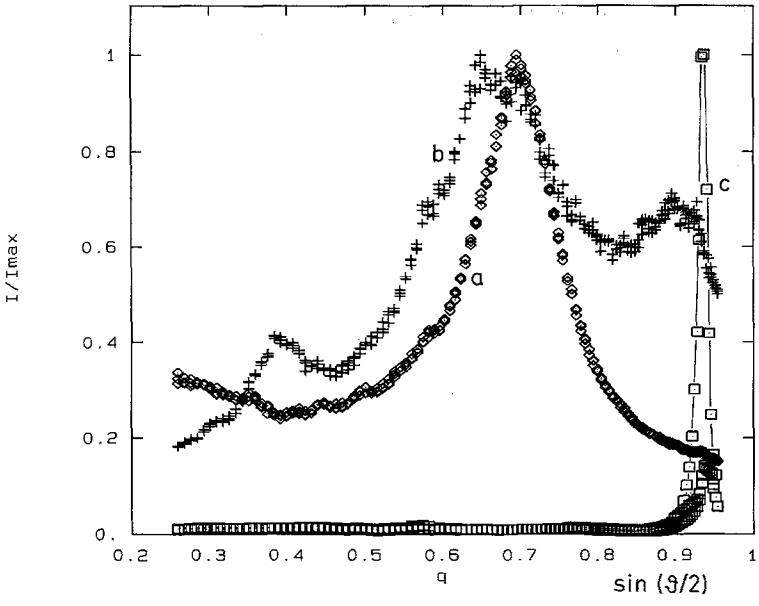

Fig. 5. Scattering behavior of solutions of 25 mM C_{12}DMAO with increasing amounts of hexanol at 25 °C Wavelength λ of the incident light: 488 nm a: 40 mM hexanol, $L_{\alpha l}$-phase b: 60 mM hexanol, L_{3m}-phase c: 95 mM hexanol, $L_{\alpha h}$-phase

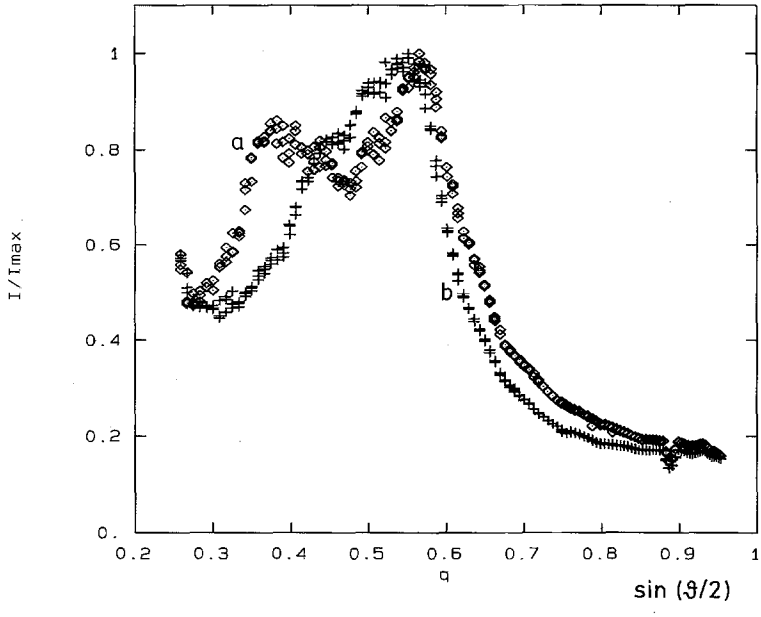

Fig. 6. Scattering behavior of the L_{3m}-region at 25 °C two months after preparation a: 15 mM C_{12}DMAO, 55 mM hexanol, L_{3m}-phase b: 15 mM C_{12}DMAO, 45 mM hexanol, (Bragg-peak is developing)

The L_{3h} phase contains some more hexanol and occurs close to the upper lamellar phase. In this L_{3h}-region a typical sponge phase can be observed. Figure 3c shows the typical structure which was found at 140 mM hexanol.

The three different lamellar regions ($L_{\alpha l}$, $L_{\alpha l-h}$ and $L_{\alpha h}$) show different textures under the polarization microscope. The textures were photographed with probes in the higher concentrated region because iridescent phases give only very weak textures which cannot be used for characterizing liquid crystalline phases. Figure 4b shows that the $L_{\alpha h}$ phase develops typical oily streaks which occur in lamellar phases only. The $L_{\alpha l}$ phase does not give such a characteristic texture (Fig. 4a) and shows strong birefringence only in a 45° position between microslide and analyzer or polarizer.

The texture of the $L_{\alpha l-h}$ region seems to be a mixture of both textures.

The electron microscopic pictures stimulated to carry out light-scattering measurements in the different regions around the iridescent phases. Figure 5 shows the angular dependence of the scattered intensity as a function of the hexanol concentration at fixed surfactant concentration of 25 mM C_{12}DMAO. The sequence of the pictures is $L_{\alpha l}$, L_{3m}, and $L_{\alpha h}$. The lower ($L_{\alpha l}$) and the upper lamellar phase ($L_{\alpha h}$) show excellent Bragg-peaks. The peak of the upper phase is much narrower than the peak of the lower lamellar phase.

The scattering behavior of the L_{3m} phases is quite different. We find extremely broad peaks (Figs. 5b and 6a). But it is very important that the main peak position is close to that of the lamellar phases. In this context it is of special interest to show that there grows a real Bragg-peak out of the L_{3m} region at a special concentration of 15 mM C_{12}DMAO and 55 mM hexanol (Fig. 6b).

Two more facts have to be mentioned. We are able to find higher order peaks in the $L_{\alpha h}$ phase only and not in the $L_{\alpha l}$ phase. The Bragg-peaks of the $L_{\alpha l}$-phase become narrower after time periods of months, whereas the peaks of the upper lamellar phase ($L_{\alpha h}$) are narrow after very short time.

4. Discussion

The L_{3l}-phase is a slightly turbid viscous phase which is optically isotropic but which shows strong flow birefringence. Electron micrographs of solutions in the L_{3l}-phase confirm the existence of particles with various sizes less than 700 nm. Since particles are not always globular, those may be unilamellar vesicles with oscillating walls which consist of C_{12}DMAO and hexanol molecules. The structure of this phase is quite different from the internal geometry of the L_{3h}-phase which appears at high hexanol concentrations. The electron micrographs clearly show the sponge structure. This sponge phase can be quickly transformed into the $L_{\alpha h}$-phase under the external stress such as flow and vibration. This experimental result shows that there is a close relationship of lamellar structures in molecular dimensions of both the L_{3h}- and the lamellar phases.

The L_{α}-phases are optically birefringent phases. Multilamellar arrangements are constructed there. The $L_{\alpha l}$-phase presents iridescence on standing for a long period, and the bright iridescence is visual in the $L_{\alpha h}$-phase which appears at higher hexanol concentrations. The interlayer distances D can be estimated from the Bragg peak position using the following equation:

$$D = \frac{\lambda_0}{2n \sin(\vartheta_{max}/2)} \quad (1)$$

$\lambda_0 = 488$ nm and n are the wavelength of the incident light and the refraction index of the solution. ϑ_{max} is the scattering angle at the peak position. The resulting D-values are 220 and 135 nm in the 30 mM and 50 mM C_{12}DMAO $L_{\alpha l}$ phases. The distances in the $L_{\alpha h}$ phase with 30 mM and 50 mM C_{12}DMAO are 165 and 103 nm [2]. Therefore, it is evident that the iridescence phenomenon is a result of the interference of light arising from the Bragg reflection between multilamellar layers, as estimated already [4–8]. The distances which were evaluated from the electronmicroscopic pictures (e.g., 190–250 nm for the $L_{\alpha h}$-phase with 30 mM C_{12}DMAO and 95 mM hexanol) are in good agreement with the light-scattering data.

The effects of undulations for the formation of multilamellar layers have already been reported [9]. The undulation maintains the average distance between lamellar sheets and conserves stably the lamellar phase. Such undulation forces are of high importance in higher concentrated lamellar phases containing electrolyte. The electronmicroscopic pictures show that there are only weak fluctuations of the lamellar surfaces in our system. These fluctuations should not be sufficient for stabilizing iridescent phases with bright colors. Yet we know that the iridescent phases containing C_{12}DMAO are stabilized by electrostatic forces due to the autoprotonation of the surfactant. Therefore, we can understand that only weak or even no fluctuations are present in the iridescent phases of our system.

It is difficult to get electronmicroscopic pictures of the $L_{\alpha l}$-region. This iridescent phase is extremely sensitive on mechanical stress. The phase transforms to L_{3m} in this case. Therefore, it is necessary to avoid that the preparation process for the electronmicroscopic pictures destroys the lamellar structure of the $L_{\alpha l}$-phase.

The slightly turbid L_{3m} phase occurs at C_{12}DMAO concentrations below 50 mM. It is optically isotropic. There are multilamellar vesicles and small lamellar fragments in this phase. It may be noted that the lamellar distance in such a vesicle is only in the order of 50 nm (at lower hexanol concentrations) and the bilayers do not oscillate. The electronmicroscopic pictures indicate that the L_{3m} phase has a structure very close to that of a lamellar phase which has been destroyed by sonication. Sonicated system forms multilamellar vesicles or very small lamellar fragments. The vesicles have no optical axis. Broken lamellar fragments are completely unordered in space. Therefore there is no macroscopic optical anisotropy. This means that no birefringence occurs in such a system.

This picture helps to understand why both the $L_{\alpha l}$-phase and the $L_{\alpha l-h}$-region are transformed by mechanical shear to phases which looks like a L_{3m}-phase. The extended lamellar structure becomes destroyed by shear rates larger than a critical value. The fragments of the broken lamellae are unordered or form multilamellar vesicles, thus diminishing the number of surfactant molecules which are at the borders of the lamellar fragments. The surfactant molecules at the borders are in a higher energetic state than the molecules inside the fragments. Therefore, the vesicle forming process is favored. It is also plausible that the size of the multilamellar vesicles should decrease with increasing shear stress.

The systems at rest transform back to lamellar phases. This process is rather fast at higher surfactant concentrations and is slowed down at lower surfactant concentrations. The reason is that the interlamellar repulsion forces which are responsible for this process decrease strongly with increasing interlamellar distances. In this way, we can understand now why the phase boundary between the L_{3m}-phase and the $L_{\alpha l-h}$-region estimated in different times after preparation of the samples moves to lower concentrations with time because parts of the L_{3m}-phase change to a lamellar phase: The L_{3m}-state is by far not thermodynamically stable in all regions.

The intensity of the scattered light as a function of the scattering angle ϑ is in accordance with this model.

Figures 5b and 6a show that the L_{3m}-phase has several very broad peaks. The mean peak position is in the region of the peak position of the lamellar phases which occur at the same surfactant concentration. We get the same scattering behavior immediately after destroying an iridescent phase by strongly shearing the solution. In both cases the light-scattering data represent lamellar fragments which are in a very unordered state or multilamellar vesicles.

The full width half maximum value of a Bragg peak is proportional to the reciprocal value of the size of the ordered lamellar regions. This means that it is not possible to simply calculate the extent of interlamellar distance fluctuations from the peak width. For example, the influence of such interlamellar distance fluctuations on the very broad peak in the $L_{\alpha l}$-phase can be completely neglected.

It is interesting that the angular dependence of the scattered light of a $L_{\alpha l}$-phase after shear or in the first weeks after preparation is quite similar to that of a L_{3m}-phase. We find a very broad peak (Fig. 7b) which becomes smaller after several months (Fig. 7c). The broad peak reflects the very small size of the undisturbed lamellar regions and distributions of different interlamellar distances in the first weeks after formation of the $L_{\alpha l}$-phase. In a very slow process these regions become larger and homogeneous, thus resulting in narrow Bragg-peaks. It is of interest that the Bragg peak is shifted to some higher interlamellar distances D during this process. The interlamellar distance changes from 213 to 234 nm. The explanation is that the total lamellar area (lamellae and holes) which gives the interlamellar distance will become somewhat smaller because the number and size of the defects in the lamellae will decrease with time. The Bragg-peaks become narrower because the size of the undisturbed lamellar regions increases during this process.

The only very narrow Bragg-peaks are found in the $L_{\alpha h}$-phase (Fig. 7a). Only this phase shows higher order peaks in light-scattering measurements. We can conclude that this phase quickly develops highly ordered lamellar regions.

The molecular lamellar structures of the $L_{\alpha l}$- and the $L_{\alpha h}$-phase should be somewhat different. The fact that, in the $L_{\alpha l}$-phase, the only strong birefringence is in a 45° position between polarizer or analyzer and glass tube has its origin in a strong, surface-forced orientation of tilted lamellae following the microscopic grooves

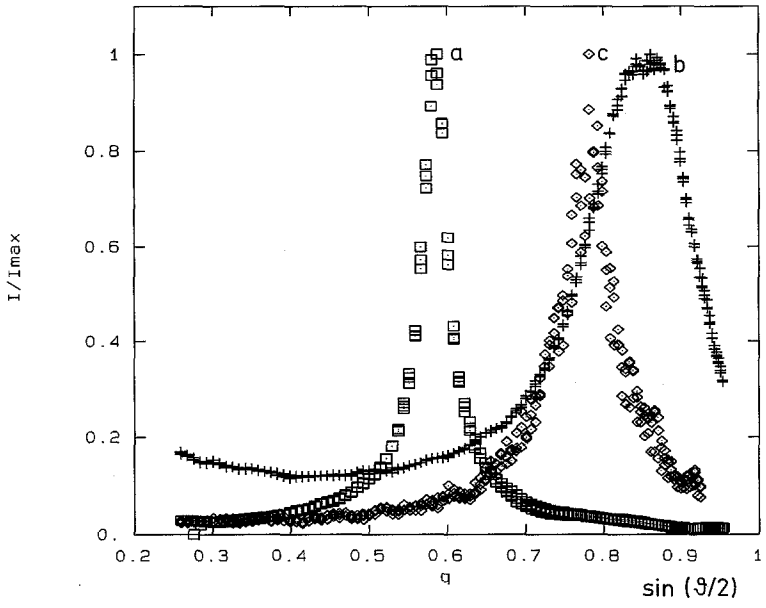

Fig. 7. Scattering behavior of the iridescent phases a: $L_{\alpha h}$ 15 mM C_{12}DMAO, 50 mM hexanol, 22 °C two days after preparation b: $L_{\alpha l}$ 30 mM C_{12}DMAO, 45 mM hexanol, 25 °C, 30 days after preparation c: $L_{\alpha l}$ 30 mM C_{12}DMAO, 45 mM hexanol, 25 °C, 6 months after preparation

inherent in the glass from manufacturing. Such domain structures have been discussed in literature [10]. Only the $L_{\alpha l}$-phase favors such biaxial orientations. Normally, we expect parallel orientations of lamellae to the glass surface which leads to psuedoisotropic orientations which give no birefringence. This is the case in the $L_{\alpha h}$-phase.

The L_{3m}-phase which is not thermodynamically stable in all regions can be understood to be a precursor of a lamellar phase. The transformation process may be so slow that no change can be observed. In other regions the process may be faster. Indeed, we observe that there grows a single and narrower Bragg-peak out of a small part of the L_{3m} phase after a long time (Fig. 6b). This means that more and more multilamellar vesicles or lamellar fragments could have condensed thus increasing the ordered lamellar region in size. The Bragg-peak is shifted to higher interlamellar distances because the total area of lamellae and holes becomes smaller.

The fact that the interlamellar distances in the multilamellar vesicles which occur at lower hexanol concentrations in the L_{3m}-region are much smaller than those of the corresponding lamellar phases shows that there is a tendency to phase separation of a more concentrated lamellar phase and a more diluted phase. This effect does not necessarily represent the position on the tie-lines which connect coexisting phases. The effect should have a kinetic origin. But it is clear that all structures we find in such a L_{3m}-phase are closely related to lamellar phases.

We conclude that the only sponge phase in our system is the L_{3h} phase. The two other isotropic phases which exhibit strong shear birefringence are a vesicle phase (L_{3l}) or a precursor of a lamellar phase (L_{3m}).

Acknowledgment

This work has been supported in part by the Nagoya University Foundation.

References

1. Platz G, Thunig C, Hoffmann H (1990) Progr Colloid Polym Sci 83:167
2. Platz G, Thunig C, Hoffmann H (1992) Ber Bunsenges Phys Chem 96(5):667–677.
3. Hoffmann H, Thunig C, Munkert U, Meyer HW, Richer W (1992) Langmuir 8:2629–2638
4. Suzuki Y, Tsutsumi H (1984) Yukagaku, 33:786
5. Satoh N, Tsuji K (1987) J Phys Chem 91:6629
6. Thunig C, Hoffmann H, Platz G (1989) Progr Colloid Polym Sci 79:297
7. Imae T, Trend B (1991) J Colloid Interface Sci 207:145
8. Imae T, Iwamoto T (1992) J Colloid Interface Sci 152:289

9. Strey R, Schomäker R, Roux D, Nallet F, Olsson U (1990) J Chem Soc Faraday Trans 86:2253
10. Gebhardt C, Gruler H, Sackmann E (1977) Z Naturforsch 32c:581–596

Received April 27, 1993;
accepted July 16, 1993

Authors' addresses:

Toyoko Imae
Department of Chemistry
Faculty of Science
Nagoya University
Chikusa
Nagoya 464, Japan

and

Gerhard Platz
Institut für Physikalische Chemie I
der Universität Bayreuth
8580 Bayreuth
FRG